

Understanding summertime H₂O₂ chemistry in North China Plain through observations and modelling studies

Can Ye¹, Pengfei Liu^{2*}, Chaoyang Xue^{3*}, Chenglong Zhang², Zhuobiao Ma², Chengtang Liu², Junfeng Liu², Keding Lu⁴, Yujing Mu^{2*}, Yuanhang Zhang⁴

¹ School of Environmental Science and Engineering, Tiangong University, Tianjin 300387, China

² Research Center for Eco-Environmental Sciences, Chinese Academy of Sciences, Beijing 100085, China

³ Max Planck Institute for Chemistry, Mainz 55128, Germany

⁴ State Key Joint Laboratory of Environment Simulation and Pollution Control, College of Environmental Sciences and Engineering, Peking University, Beijing, 100871, China

Correspondence to: Pengfei Liu (pfliu@rcees.ac.cn), Chaoyang Xue (ch.xue@mpic.de), Yujing Mu (yjmu@rcees.ac.cn)

Abstract.

Hydrogen peroxide (H₂O₂) is a key atmospheric oxidant, crucial for oxidation capacity and sulfate production. However, its chemistry remains understudied compared to ozone (O₃), limiting our understanding of photochemical pollution. In summer 2016, atmospheric peroxides and trace gases were measured at a rural site in the North China Plain. H₂O₂ was the dominant peroxide (0.62±0.800.62 ppb), constituting 69% of total peroxides. It exhibited diurnal variation similar to peroxyacetyl nitrate (PAN) and O₃, indicating photochemical production. The O₃/H₂O₂ ratio was higher on high-particle days, suggesting H₂O₂ uptake by particles reduces its concentration. A box model with default gas-phase chemistry overestimated H₂O₂ by a factor of 2.7, and including particle uptake of H₂O₂ (uptake coefficient: 6×10⁻⁴) improved agreement with observations, although we note this value carries some uncertainty related to the assumed HO₂ uptake coefficient.~~A box model with default gas-phase chemistry overestimated H₂O₂ by a factor of 2.7, but including particle uptake (uptake coefficient: 6×10⁻⁴) improved agreement with observations.~~

HO₂ recombination contributed 91% of H₂O₂ production, with a peak rate of 1 ppb h⁻¹. Major removal pathways included particle uptake (69%), dry deposition (25%), OH reaction (4%), and photolysis (2%). Relative incremental reactivity (RIR) analysis showed that reducing NO_x, PM_{2.5}, and alkanes increased H₂O₂, while reducing alkenes, aromatics, CO, and HONO decreased it, with alkenes having the strongest effect. H₂O₂/NO_z ratios (>0.15 in 82% of cases) indicated O₃ formation was in a transition and NO_x-sensitive regime, emphasizing the need for VOC and further NO_x reductions to mitigate both H₂O₂ and O₃ pollution. These findings improve our understanding of H₂O₂ chemistry and provide insights for mitigating photochemical pollution in rural North China.

The atmospheric oxidation capacity is a critical determinant of atmospheric self-cleaning, influencing the residence time and persistence of pollutant gases. Quantifying this capacity is essential for elucidating the lifetimes of pollutants, the formation of aerosols, and their subsequent radiative forcing effects. Hydrogen peroxide (H_2O_2) serves as a significant atmospheric oxidant, primarily generated through the recombination of hydroperoxyl radicals (HO_2), which are themselves derived from reactions involving hydroxyl radicals (OH), volatile organic compounds (VOCs), and carbon monoxide (CO). Consequently, the formation of H_2O_2 is intrinsically linked to atmospheric oxidation capacity, with its concentration serving as a direct indicator of the intensity of this capacity. Furthermore, as H_2O_2 represents a terminal product in the ozone (O_3) formation chain reaction, its concentration can be utilized to assess the sensitivity of O_3 production to precursors (Sillman, 1995; Reeves and Penkett, 2003; Nunnermacker et al., 2008; He et al., 2010). Owing to its strong oxidative potential and high Henry's law constant, H_2O_2 readily dissolves in cloud droplets, where it oxidizes sulfur dioxide (SO_2) to form sulfuric acid (H_2SO_4), thereby contributing to sulfate aerosol formation and acid rain deposition (Calvert et al., 1985). Research indicated that H_2O_2 -mediated oxidation of SO_2 in cloud water accounts for 60-80% of global SO_2 oxidation (Penkett et al., 1979; Calvert et al., 1985; Sofen et al., 2011). Additionally, recent studies have highlighted the significant role of particle-phase H_2O_2 oxidation in sulfate formation during winter (Ye et al., 2018; Ye et al., 2021b; Gao et al., 2024). Given its potent oxidative properties, H_2O_2 also poses substantial risks to human health and vegetation (Chen et al., 2010). Thus, a precise understanding of H_2O_2 chemistry is imperative for advancing knowledge of atmospheric oxidation processes and for diagnosing underlying secondary pollution formation mechanisms.

Atmospheric H_2O_2 concentrations are currently reported to range from 0.1 to 13 ppb (Balasubramanian and Husain, 1997; Walker et al., 2006; Ren et al., 2009; Guo et al., 2014; He et al., 2010; Qin et al., 2018; Fischer et al., 2015; Fischer et al., 2019; Ye et al., 2022; Allen et al., 2022; Zhang et al., 2018), with their spatial and temporal variability governed by a balance between production sources and removal pathways. H_2O_2 is generated through both primary and secondary sources. Primary sources of H_2O_2 include biomass burning, which can contribute substantially under specific conditions. For instance, Ye et al. (2022) reported elevated H_2O_2 concentrations during biomass combustion events, which promote secondary sulfate formation and thereby increase fine particulate matter ($\text{PM}_{2.5}$) concentrations. The dominant secondary source is the recombination of HO_2 radicals, a process enhanced during summer months due to increased solar radiation, which elevates HO_2 concentrations and consequently leads to higher H_2O_2 levels. However, under elevated nitrogen oxide (NO_x) conditions, nitric oxide (NO) reacts competitively with HO_2 , suppressing H_2O_2 formation and resulting in reduced atmospheric concentrations. Another secondary source involves the ozonolysis of alkenes, which produces Criegee intermediates that can decompose to form H_2O_2 (Becker et al., 1990). This pathway is particularly relevant during nighttime and potentially in winter, when photochemical activity is diminished (Lee et al., 2008b). For example, alkene ozonolysis was found to dominate wintertime H_2O_2 levels (>70%) (Qin et al., 2018), although the yields are generally low, often below 10%.

Additionally, the release of H_2O_2 from the particle phase has been proposed as a potential source, though its contribution is considered negligible compared to gas-phase production. Recent studies, however, have highlighted that under polluted
65 conditions, high concentrations of humic-like substances and transition metals can facilitate particle-phase H_2O_2 formation, which subsequently partitions into the gas phase, significantly enhancing gas-phase H_2O_2 levels (Ye et al., 2021b; Liu et al., 2021).

H_2O_2 can be removed by photolysis, which not only depletes H_2O_2 but also serves as a source of hydroperoxyl radicals
70 (HOx). However, due to lower photolysis frequency, the contribution of H_2O_2 photolysis to atmospheric HOx production is generally much smaller compared to photolysis of O_3 , nitrous acid (HONO), and formaldehyde (HCHO). Notably, particle-phase H_2O_2 photolysis has been identified as a critical source of free radicals within aerosols, accelerating aerosol aging and promoting the formation of secondary pollutants. Rao et al. (2023) further emphasized a significantly accelerated rate for air-water interface H_2O_2 photolysis, underscoring its importance as a source of particle-phase OH . Dry deposition is another key
75 removal mechanism, leading to a vertical gradient in H_2O_2 concentrations, with peak levels observed at approximately 2 km above the surface (Watanabe et al., 2016; Klippel et al., 2011). Due to its high solubility, wet deposition through rainwater scavenging also effectively removes H_2O_2 from the atmosphere. Moreover, laboratory and field studies have demonstrated that heterogeneous uptake by particles can significantly contribute to H_2O_2 removal under polluted conditions. Qin et al. (2022) reported a maximum uptake coefficient of 2.49×10^{-3} for H_2O_2 by ambient particles, with the uptake coefficient
80 influenced by the concentration of transition metals within the particles.

In addition to H_2O_2 , the atmosphere contains a variety of organic peroxides, such as methyl hydroperoxide (CH_3OOH), formed through reactions between HO_2 and organic peroxy (RO_2) radicals. While H_2O_2 is the most abundant peroxide in the atmosphere, organic peroxides are recognized as a significant component of secondary organic aerosol (SOA), contributing
85 to aerosol composition and properties. However, due to analytical challenges associated with measuring organic peroxides, most studies on atmospheric peroxides have only focused on H_2O_2 (Zhang et al., 2012).

Photochemical pollution has emerged as a critical air quality issue in China, impacting both urban and rural regions. H_2O_2 and O_3 are key products of photochemical pollution, and elucidating their chemical behavior is essential for developing
90 effective strategies to mitigate photochemical pollution. However, compared to the extensive research on O_3 , studies on H_2O_2 remain limited due to the technical challenges and complexities associated with its measurement. In recent years, O_3 concentrations in the North China Plain have exhibited a significant upward trend (Li et al., 2019; Wang et al., 2020; Lu et al., 2020), yet the characteristics of H_2O_2 in this region remain poorly understood. Furthermore, the implementation of national emission reduction policies has led to a substantial decline in NOx , while VOCs persist at elevated levels (Liu et al.,
95 2023). This shift toward low NOx and high VOCs conditions is more conducive to H_2O_2 formation. Although photochemical pollution is traditionally considered as an urban phenomenon, recent studies have highlighted its increasing prevalence in

rural areas, where pollution levels are gradually approaching those observed in urban areas (Ma et al., 2016). Rural regions typically exhibit lower NO_x concentrations than urban areas, creating conditions more favorable for H₂O₂ production. Despite this, research on H₂O₂ in rural areas of the heavily polluted North China Plain remains scarce. Consequently, there is an urgent need to investigate H₂O₂ chemistry in rural environments to inform targeted control strategies for photochemical pollution.

This study is based on a field campaign conducted in a rural area of the North China Plain, during which a comprehensive suite of gaseous (including H₂O₂), particulate matter, and meteorological parameters, were measured. Here we investigate the temporal variations of H₂O₂, and its relationships with other oxidants (e.g., O₃ and peroxyacetyl nitrate, PAN), and preliminarily estimate organic peroxide concentrations. A zero-dimensional box model was employed to examine the influence of particles on the H₂O₂ budget and the sensitivity of H₂O₂ production to various chemical species. Finally, we explore the potential of H₂O₂ as an indicator for determining O₃ sensitivity and discuss the control strategy for alleviating photochemical pollution.

2 Experiments

2.1 Measurement site

The observational experiment was conducted at the Station of Rural Environment, Research Center for Eco-Environmental Sciences (SRE-RCEES, 38°42'N, 115°15'E), located in Dongbaituo Village, Wangdu County, Hebei Province. Situated approximately 180 km southwest of Beijing, the station is surrounded primarily by farmland with no nearby industrial facilities, making it an ideal site for studying typical rural atmospheric conditions. This location has historically served as a key site for numerous large-scale observational campaigns (Tan et al., 2017; Peng et al., 2021). The experiment took place from 6 July 2016 to 12 August 2016, with the primary objective of investigating the underlying causes of photochemical pollution in the rural North China Plain.

2.2 H₂O₂ measurements

H₂O₂ concentrations were measured using the AL-2021 H₂O₂ monitor (Aero-Laser) (Lazrus et al., 1986). The instrument operates on the following principle: gas-phase peroxides in ambient air are collected by buffered solution in a glass stripping coil. The trapped peroxides then react with p-hydroxyphenyl acetic acid (POPHA) under the catalysis of peroxidase, producing a fluorescent dimer. This dimer exhibits maximal light absorption at a characteristic wavelength of 320 nm and emits fluorescence with a central wavelength of 400 nm. By continuously monitoring the intensity of this fluorescence signal, the instrument enables online quantitative detection of atmospheric peroxides. To differentiate between H₂O₂ and organic peroxides, a dual-channel measurement approach was employed. Channel A measures the total peroxide content, while Channel B incorporates catalase into the absorbent solution to selectively decompose H₂O₂, thereby measuring only organic

peroxides. The H₂O₂ concentration is determined by the difference in signals between the two channels. Although Channel A provides an approximation of ~~total-atmospheric~~ organic peroxides, it is important to note that the percentage of organic peroxides reported in this study represents a lower limit, as the collection efficiency of the stripping coil technique varies significantly among different organic peroxide species. While H₂O₂ is efficiently trapped due to its high solubility (Henry's law constant: $\sim 10^5$ M atm⁻¹), many organic peroxides such as methyl hydroperoxide (MHP) have substantially lower solubilities (Henry's law constant: 3×10^2 M atm⁻¹), resulting in lower collection efficiencies. Additionally, the catalase used to differentiate between H₂O₂ and organic peroxides may not completely discriminate between certain hydroperoxide species, further contributing to uncertainty in organic peroxide quantification. ~~it should be noted that not all organic peroxides are as efficiently absorbed as H₂O₂, resulting in an underestimation of total organic peroxide concentrations.~~ The detection limit of the H₂O₂ measurement instrument is 50 ppt, with an uncertainty of 10%. To ensure the stability of the instrument's operation, regular calibrations are performed at fixed intervals. In several previous field experiments (Ye et al., 2018; Ye et al., 2021b; Ye et al., 2021a; Liu et al., 2021), this instrument has been successfully utilized to measure atmospheric H₂O₂, demonstrating high reliability and consistent operational stability.

2.3 Other species

NO_x, O₃, SO₂, PM_{2.5}, CO, and total reactive nitrogen (NO_y) were measured using commercial instruments from Thermo Electron. Volatile organic compounds (VOCs) were quantified by gas chromatography with a flame ionization detector (GC-FID), while nitrous acid (HONO) was measured using a long-path absorption photometer (LOPAP) from QUMA. The aerosol surface area density was calculated by combining data from a scanning mobility particle sizer (SMPS) and an aerodynamic particle sizer (APS). PAN was analyzed using gas chromatography with electron capture detection (GC-ECD). Gas-phase meteorological data were collected using a portable meteorological station (Model WXT520, Vaisala, Finland). The photolysis rate constant of NO₂ ($j(\text{NO}_2)$) was measured directly, and other photolysis rate constants were derived using the Tropospheric Ultraviolet and Visible (TUV) radiation model, scaled based on $j(\text{NO}_2)$ measurements. Detailed information on the experimental instruments is provided in Table S1.

2.4 Box model descriptions

A zero-dimensional box model based on the RACM2-LIM1 mechanism was employed to investigate the sources and removal mechanisms of H₂O₂. This model is widely recognized for its ability to accurately model HO_x radicals (Tan et al., 2017; Ma et al., 2022). Given that the HO₂ is a critical precursor for H₂O₂ formation, the model's strong performance in simulating free radicals provides confidence in its ability to reliably simulate H₂O₂ concentrations. The model was constrained using input parameters including photolysis rate constants ($j(\text{NO}_2)$, $j(\text{O}^1\text{D})$, $j(\text{HONO})$, $j(\text{H}_2\text{O}_2)$, $j(\text{HCHO})$), VOCs, NO, NO₂, O₃, HONO, methane (CH₄), CO, and meteorological data (temperature, relative humidity, and pressure). VOCs were categorized into different reactivity-based groups according to their reaction rates with OH, as detailed in Table S2.

The dry deposition rate constant for H₂O₂ was set to 3×10⁻⁵ s⁻¹, and boundary layer heights were derived from the hybrid single-particle ~~lagrangian~~-Lagrangian integrated trajectory (HYSPLIT) model.

The simulation focused on the period from 24 July to 3 August, selected for its stable meteorological conditions, characterized by low wind speeds and predominantly static weather. During this period, the observed trends in H₂O₂ concentrations exhibited consistent patterns, suggesting that local photochemical processes were the primary source of H₂O₂. This makes the selected timeframe ideal for exploring H₂O₂ sources using the box model. Additionally, elevated PM_{2.5} concentrations during this period provided an opportunity to investigate the potential influence of particle uptake on H₂O₂ removal. The rate coefficient of H₂O₂ uptake by particles was parameterized as equation 1:

$$k=0.25 \times c \times \gamma \times S_a \quad \text{Eq. 1}$$

Here c is mean molecular speed of H₂O₂, γ is the H₂O₂ uptake coefficient, and S_a is aerosol surface area density.

To assess the contributions of different precursors to H₂O₂ production, Relative Incremental Reactivity (RIR) analysis was conducted. RIR was calculated using the following equation:

$$\text{RIR}(X) = \frac{\frac{\Delta H_2O_2(X)}{H_2O_2}}{\frac{\Delta C(X)}{C(X)}} \quad \text{Eq. 2}$$

In Eq.2, X represents the primary pollutants that may influence H₂O₂ concentrations. H₂O₂ represents modelled H₂O₂ in the base case. ΔC(X)/C(X) represents the relative change of primary pollutants. ΔH₂O₂(X)/H₂O₂ represents the relative change of modelled H₂O₂ concentrations induced by the reduction of X. Considering the variations in simulated radical concentrations and the deviations in the RIR, a 20% reduction scenario was selected for further analysis. This approach allowed for the quantification of the sensitivity of H₂O₂ production to variations in precursor concentrations, providing insights into the key drivers of H₂O₂ formation in the rural North China Plain.

3 Results and discussion

3.1 Time series overview

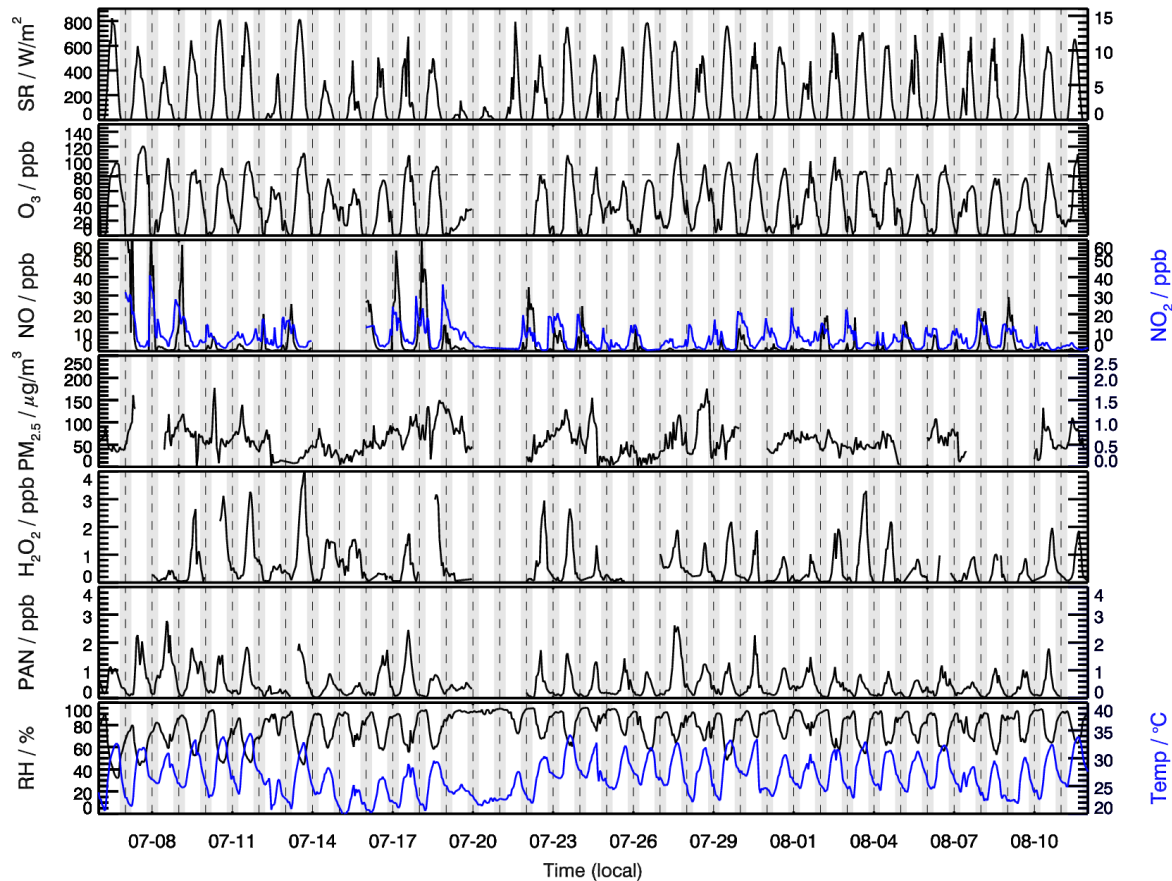


Figure 1. Measurements of H₂O₂, other related chemical species and meteorological parameters at SRE-RCEES site during the observation period.

180

185

Throughout the observation period, meteorological conditions were characterized by high temperature and relative humidity. High temperature generally increased the rate constants of photochemical reactions, while abundant water vapor enhanced the recombination rate of HO₂ and the reaction rate between O(¹D) and water vapor (H₂O). The maximum O₃ concentration reached 120 ppb, with the maximum daily 8-hour average (MDA8) frequently exceeding the National Ambient Air Quality Standard (NAAQS) Class-II standard of 82 ppb (25 °C, 1013 kPa). High O₃ pollution events often coincided with elevated H₂O₂ concentrations (>2 ppb), suggesting that O₃ production at this site may be sensitive to NO_x. This hypothesis will be further investigated using the H₂O₂/NO_x and O₃/NO_x in Section 3.6 on O₃ sensitivity. NO_x concentrations peaked in the morning, driven by factors such as traffic emissions and lower boundary layer height. Daytime NO concentrations were generally below 1 ppb, while daily peak H₂O₂ concentrations exhibited significant day-to-day variability, ranging from

190 approximately 0.2 ppb to 4 ppb. Higher H₂O₂ concentrations were observed during periods of intense solar radiation, indicating that local photochemical reactions play a significant role in H₂O₂ production. Notably, elevated H₂O₂ levels were only observed when NO concentrations were low, consistent with the known mechanism of H₂O₂ formation under low NO_x conditions.

195 The average H₂O₂ concentration during the whole observation period was 0.62±0.80 ppb, significantly higher than wintertime concentrations (0.19 ppb) at the same site (Ye et al., 2021b), as summer conditions with high solar radiation intensity and relative humidity are more conducive to H₂O₂ production. This average concentration also exceeded summer H₂O₂ levels reported in urban areas, such as Beijing (0.27 pb) (Qin et al., 2018) and ~~Hongkong-Hong Kong~~ (0.32 ppb) (Guo et al., 2014), likely due to lower NO_x levels at the rural site, which favor H₂O₂ formation. Compared to H₂O₂ concentrations
200 reported at rural sites in other countries, the levels observed in this study were lower than that in Kinterbish (Watkins et al., 1995), Whiteface Mountain (1.61 ppb) (Balasubramanian and Husain, 1997). It is worth mentioning that, an average H₂O₂ concentration of 0.51±0.90 ppb was reported at the same site in summer 2014 (Wang et al., 2016), lower than the current study's findings, reflecting a potential increasing trend in H₂O₂ concentrations over time. In addition, multi-year measurements at the summit of Mount Tai revealed an increasing trend of H₂O₂ concentrations in cloud water from 2014 to
205 2018 (Li et al., 2020), indirectly indicating rising gas-phase H₂O₂ levels in the North China Plain. The significant reduction in NO_x emissions in the North China Plain over recent years, while VOC levels remained relatively high or decreased less sharply, has likely shifted the atmospheric chemistry towards conditions more favorable for HO₂ recombination, potentially contributing to the observed increasing trend in H₂O₂ concentrations. This aligns with the known sensitivity of H₂O₂ formation to NO_x levels.

210 Elevated H₂O₂ concentrations and high relative humidity in rural areas facilitate the oxidation of SO₂ by H₂O₂ in both aerosol water and cloud water, contributing to sulfate formation and increased PM_{2.5} levels. During the observation period, the average PM_{2.5} concentration reached 57 µg m⁻³, and the co-occurrence of PM_{2.5} and O₃ pollution was frequently observed. This dual pollution phenomenon suggests that high concentrations of oxidants may play a significant role in driving
215 secondary aerosol formation. PAN, another key secondary oxidant measured in this study, reached a maximum concentration of 2.9 ppb. Similar to H₂O₂ and O₃, PAN is a product of photochemical pollution, and its temporal trends closely mirrored those of H₂O₂ and O₃. These trends will be analyzed in detail in the section 3.2. As strong oxidizing agents, H₂O₂, O₃ and PAN are proven to be damaging to vegetation and human health. Given the high concentrations of these oxidants observed in this study, photochemical pollution in rural areas poses serious risks to agricultural productivity and human health.

220 3.2 Diurnal patterns of three photochemical oxidants

The average diurnal trends of H₂O₂, PAN, and O₃ exhibited pronounced daily variations, with concentrations peaking during the daytime and declining at night (Figure 2). These trends closely followed solar radiation patterns, highlighting the

significant contribution of photochemical reactions to their formation. In addition, the pronounced daily variations also indicated the presence of abundant precursors in the region facilitating the production of H₂O₂, PAN, and O₃. In the early morning, as solar radiation intensified, the photolysis of HONO initiated daytime photochemical reactions (R0), generating peroxy radicals (R1). These radicals reacted with NO to produce O₃ (R2-R5); HO₂ recombination underwent bimolecular recombination to produce H₂O₂ (R6); peroxyacetyl radicals (PA) reacted with NO₂ to form PAN (R7). These processes led to a rapid increase in the concentrations of all three oxidants, with peak concentrations reaching 1.8 ppb, 1.2 ppb, and 84 ppb for H₂O₂, PAN, and O₃, respectively.

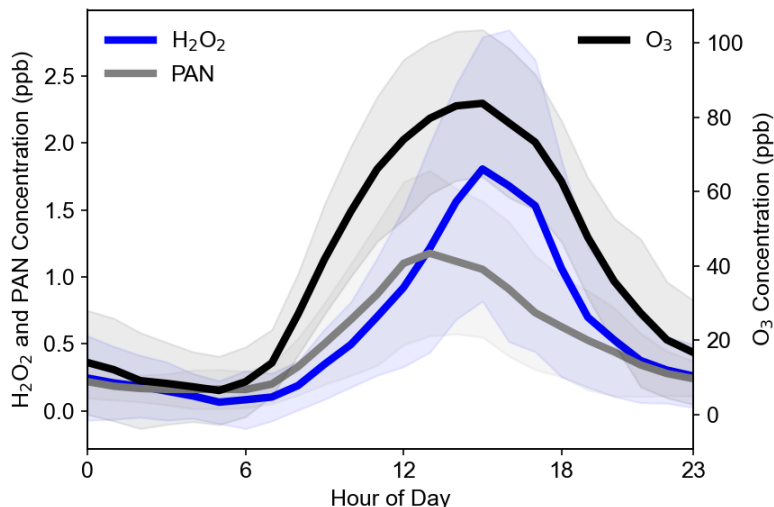
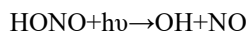


Figure 2. Diurnal cycles of H₂O₂, PAN and O₃.

Despite sharing similar photochemical formation pathways, the peak times of the three oxidants differed due to variations in their production and removal rates. PAN concentrations peaked around noon, approximately 2–3 hours earlier than H₂O₂ and O₃, a phenomenon also observed in previous studies (Lee et al., 2008a). This earlier peak for PAN can be attributed to its higher thermal decomposition rate at midday. In contrast, the peaks for H₂O₂ and O₃ both occurred around 16:00. Notably, in urban areas, H₂O₂ peaks often lag behind O₃ peaks. For example, observations at the urban Tai'an site in the North China Plain revealed that H₂O₂ peaks occurred approximately 2 hours after O₃ peaks (Ye et al., 2021a). This delay can be explained by HO₂ chemistry under varying NO_x conditions. Under high NO_x condition, HO₂ primarily reacts with NO (reaction rate constant: $8.9 \times 10^{-12} \text{ cm}^3 \text{ molecule}^{-1} \text{ s}^{-1}$ at 298 K), whereas under low NO_x condition, HO₂ undergoes bimolecular recombination to form H₂O₂ (reaction rate constant: $1.5 \times 10^{-12} \text{ cm}^3 \text{ molecule}^{-1} \text{ s}^{-1}$ at 298 K). In urban settings, H₂O₂ peaks only occur when NO concentrations drop to around 100 ppt, allowing HO₂ recombination to dominate, thus delaying the H₂O₂ peak relative to O₃. However, at this rural site, daytime NO concentrations were consistently low, resulting in simultaneous peaks for O₃ and H₂O₂.



R0



245

Following their peaks, the concentrations of all three oxidants declined rapidly. For H_2O_2 , this decrease was primarily driven by dry deposition and, in the evening, enhanced uptake by liquid aerosols formed as relative humidity increased. O_3 concentrations dropped due to a combination of dry deposition and NO titration, while PAN levels decreased mainly through thermal decomposition. At night, the absence of photochemical reactions caused all three oxidants to maintain low concentrations.

250

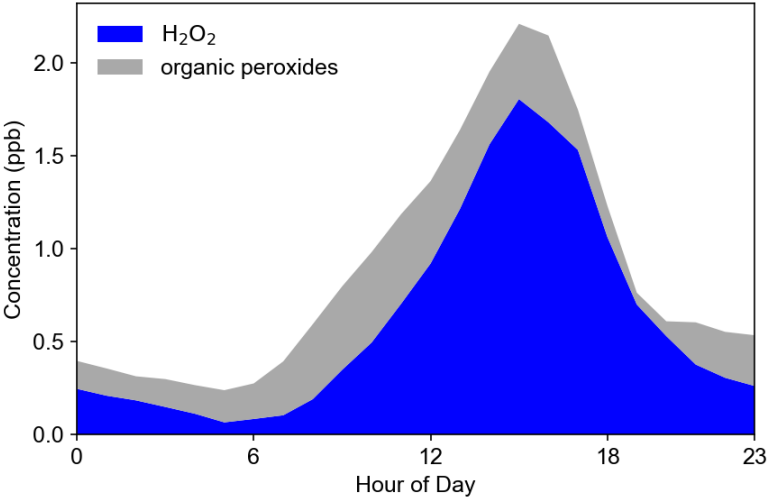


Figure 3. The concentrations of H_2O_2 and organic peroxides.

255

Figure 3 illustrates the average diurnal trends of organic peroxides and H_2O_2 . The trends of total peroxides closely align with those of H_2O_2 , indicating similar production and removal mechanisms. H_2O_2 accounts for 69% of the total peroxides on average, while organic peroxides (0.28 ppb) constitute 31%. This demonstrates that peroxides in rural areas are predominantly dominated by H_2O_2 , consistent with the findings of Wang et al. (2016) at this site. However, it is important to note that the percentage of organic peroxides reported in this study represents a lower limit, as not all organic peroxides are fully captured by the measurement technique. In contrast, Liang et al. (2013) reported that organic peroxides accounted for 80% of total peroxides in urban areas such as Beijing. The difference in organic peroxide proportions between Beijing and

260

Wangdu can likely be attributed to variations in chemical conditions, such as differences in VOC compositions, which influence the types and abundances of peroxy radicals formed.

The diurnal variation in the relative contributions of H_2O_2 and organic peroxides to total peroxides, reflects their distinct production and loss mechanisms. H_2O_2 dominates (over 90%) around 19:00 due to strong photochemical production via HO_2 recombination during the day, while its contribution drops to ~25% by 05:00 due to nighttime losses (e.g., heterogeneous uptake and dry deposition) without replenishment. In contrast, organic peroxides contribute more significantly in the early morning, likely due to slower loss rates compared to H_2O_2 . Organic peroxides such as CH_3OOH (methyl hydroperoxide) have much lower dry deposition rates—approximately 30 times lower than that of H_2O_2 —leading to less nighttime loss and a higher relative contribution to total peroxides during early morning hours. These differences highlight the distinct photochemical dynamics and loss mechanisms of H_2O_2 compared to organic peroxides, influenced by diurnal variations in radiation, precursor concentrations, and meteorological conditions.

3.3 Correlations between different atmospheric oxidants

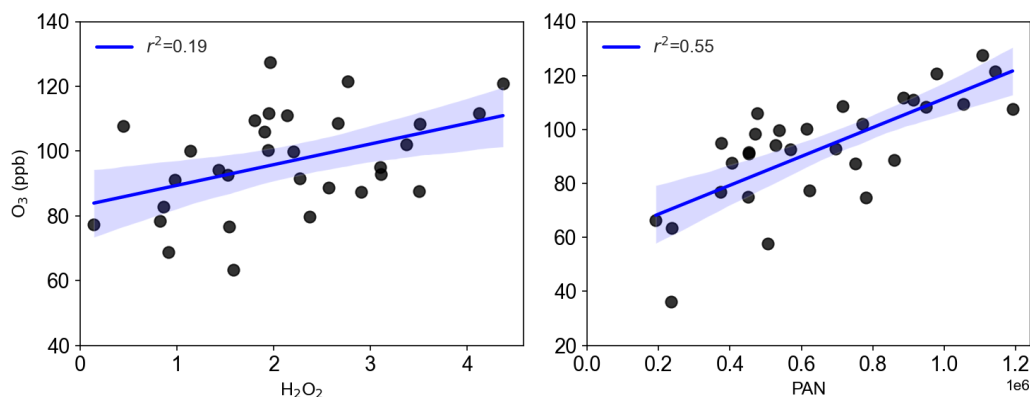


Figure 4. Correlations of O_3 daily maximum with H_2O_2 and PAN daily maximum

The formation of H_2O_2 , O_3 , and PAN is closely linked to VOCs, NO_x , and solar radiation. Consequently, their concentrations are typically elevated and well-correlated during photochemical pollution episodes. Here, we investigate the relationships among these oxidants. Figure 4 illustrates the correlations between the daily maximum concentrations of H_2O_2 , O_3 , and PAN. A good correlation ($r^2=0.55$) was observed between PAN and O_3 , consistent with previous studies (Lee et al., 2008a; Zhang et al., 2014; Xu et al., 2021; Sun et al., 2020). In contrast, the correlation between H_2O_2 and O_3 was weak ($r^2=0.19$). Prior research has shown positive correlations between H_2O_2 and O_3 during photochemical pollution due to their shared dependence on VOC and NO_x photochemistry (Hua et al., 2008; Takami et al., 2003; Ye et al., 2021a; Guo et al., 2022), while negative correlations have been reported in clean marine boundary layer where O_3 photolysis dominates radical production (Ayers et al., 1992). The lack of a positive correlation between O_3 and H_2O_2 in this rural polluted environment may indicate additional factors influencing H_2O_2 concentrations. Notably, heterogeneous uptake by particles has been shown

to affect H_2O_2 levels (De Reus et al., 2005; Qin et al., 2018), and given the relatively high $\text{PM}_{2.5}$ concentrations during the observation period, we hypothesize that heterogeneous loss reduces gas-phase H_2O_2 , weakening its correlation with O_3 . Additionally, aqueous-phase reactions in aerosol water or cloud droplets, facilitated by high relative humidity during the campaign, could further reduce gas-phase H_2O_2 without affecting O_3 , contributing to the decoupling of their peak values. While the focus on daytime maxima limits the direct relevance of nighttime chemistry, processes such as alkene ozonolysis or nocturnal deposition could influence background H_2O_2 levels, indirectly affecting daytime peaks.

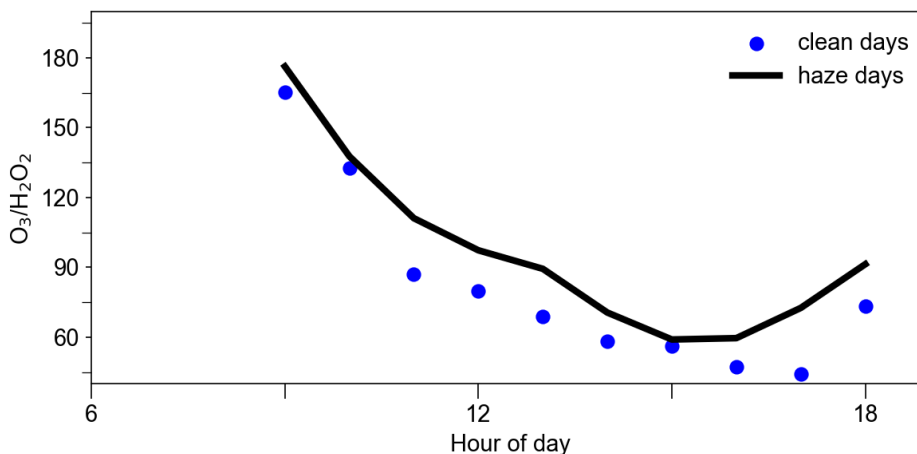


Figure 5. Average $\text{O}_3/\text{H}_2\text{O}_2$ from 9:00 to 18:00 on clean (daily average $\text{PM}_{2.5} < 50 \mu\text{g m}^{-3}$) and polluted days (daily average $\text{PM}_{2.5} \geq 50 \mu\text{g m}^{-3}$).

To test this hypothesis, we analyzed the $\text{O}_3/\text{H}_2\text{O}_2$ ratio on polluted (daily average $\text{PM}_{2.5} < 50 \mu\text{g m}^{-3}$) and clean days (daily average $\text{PM}_{2.5} \geq 50 \mu\text{g m}^{-3}$). While O_3 and H_2O_2 share similar photochemical formation pathways, O_3 is less affected by particle uptake. O_3 lifetime was estimated to be 13 days with respect to heterogeneous uptake for dust mass concentrations of $1000 \mu\text{g m}^{-3}$, highlighting the minor role of particle uptake on O_3 removal (Tang et al., 2017). If the $\text{O}_3/\text{H}_2\text{O}_2$ ratio remains stable across polluted and clean conditions, heterogeneous uptake likely has minimal impact on H_2O_2 . However, if the ratio is higher during polluted periods, it is possible that $\text{PM}_{2.5}$ may scavenge H_2O_2 by heterogeneous uptake. As shown in Figure 5, the $\text{O}_3/\text{H}_2\text{O}_2$ ratio during peak photochemical hours (9:00–18:00) was markedly higher on polluted days compared to clean days, supporting the hypothesis that heterogeneous uptake by $\text{PM}_{2.5}$ significantly reduces H_2O_2 concentrations. It is important to note that this method provides only a preliminary assessment, as uncertainties exist due to differences in the dependence of H_2O_2 and O_3 on peroxy radical concentrations and their respective responses to radiation intensity. In addition, differences in photochemical regimes, potentially driven by varying VOC/NOx ratios between clean and polluted days, could also influence the $\text{O}_3/\text{H}_2\text{O}_2$ relationship independently of particle uptake effects. In the following section, we further examine the impact of $\text{PM}_{2.5}$ on H_2O_2 budget using a box model.

3.4 Investigation on H₂O₂ budget

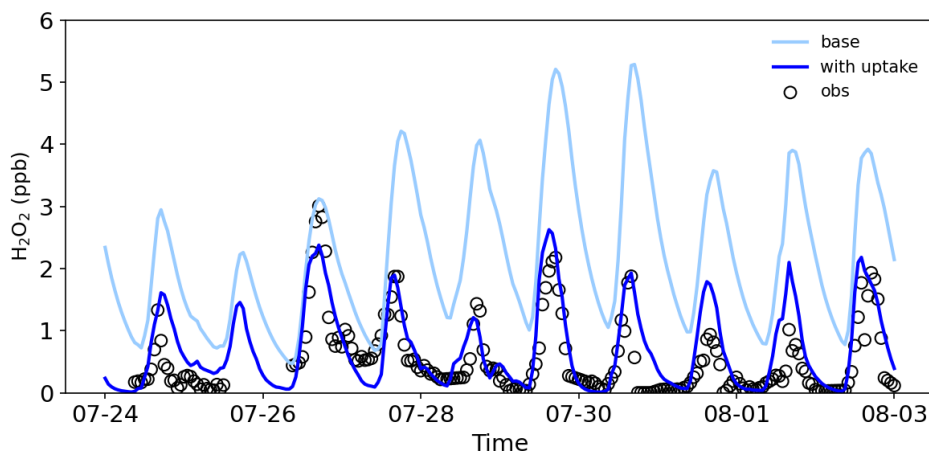


Figure 6. Observed and modelled H₂O₂ concentrations from 24 July to 3 August.

To better understand the sources and removal mechanisms of H₂O₂, we employed a box model to simulate its concentrations. As shown in Figure 6, base simulations using the model's default H₂O₂ source and removal mechanisms overestimated H₂O₂ concentrations compared to observations, with a simulated-to-measured ratio of 2.7. This discrepancy suggests an unaccounted removal pathway, consistent with our earlier hypothesis of H₂O₂ removal by particle uptake. When a parameterized uptake mechanism with an uptake coefficient of 6×10^{-4} was incorporated into the box model, the simulated H₂O₂ concentrations and trends aligned well with observed values (Fig. 6), confirming the significant role of particle uptake in H₂O₂ removal in rural areas. This uptake coefficient is comparable with the value (5×10^{-4}) estimated during a dense Saharan dust event (De Reus et al., 2005), and lower than 1×10^{-3} reported by Wang et al. (2016), which may be likely due to differences in particulate matter composition. Sensitivity tests indicated that an uptake coefficient of 1×10^{-3} resulted in underestimation (Figure.S1), supporting 6×10^{-4} as the optimal value for our study. This coefficient falls within the range (10^{-4} - 10^{-3}) determined in laboratory studies for H₂O₂ uptake on ambient particles collected on filters or artificial particles (Pradhan et al., 2010; Romanias et al., 2012; Qin et al., 2022). We believe this value represents a reasonable estimate for the conditions at our sampling site, though we acknowledge that a more dynamic treatment of heterogeneous processes that accounts for variations in aerosol composition, phase state, and ambient RH would be valuable in future studies.

It should be mentioned that previous studies have demonstrated that considering HO₂ by particles can partially explain the discrepancy between observed and modeled HO₂ concentrations under low NO_x conditions (Kanaya et al., 2007a; Kanaya et al., 2007b; Whalley et al., 2010; Ma et al., 2022), as well as the phenomenon of increasing O₃ concentrations with decreasing particulate matter levels (Li et al., 2019). Since HO₂ is a precursor to H₂O₂, its uptake by particles naturally reduces H₂O₂ concentrations. However, laboratory-measured HO₂ uptake coefficients exhibit significant variability, ranging from 10^{-5} to 0.82, and are strongly influenced by the composition of particulate matter (Thornton et al., 2008; Taketani et al., 2012;

George et al., 2013; Lakey et al., 2015). Through analysis of measured radical budget and related parameters, Tan et al. (2020) showed that the HO₂ uptake was not important in the North China Plain in 2014, with an uptake coefficient of 0.08. Given that our observational experiments were conducted at the same site with similar particulate matter composition, we also assumed an HO₂ uptake coefficient of 0.08 to investigate its impact on the H₂O₂ budget. Under this assumption, we found that an H₂O₂ uptake coefficient of 4.5×10^{-4} resulted in a good agreement between modeled and observed H₂O₂ concentrations (Figure S1). The results indicate that considering HO₂ uptake reduces the H₂O₂ uptake coefficient by 25%. Therefore, uncertainties in the HO₂ uptake coefficient significantly affect the accurate simulation of H₂O₂ concentrations and the estimation of the H₂O₂ uptake coefficient. A more precise parameterization scheme for HO₂ uptake is critical for models to accurately assess the global distribution of H₂O₂ concentrations and their environmental impacts.

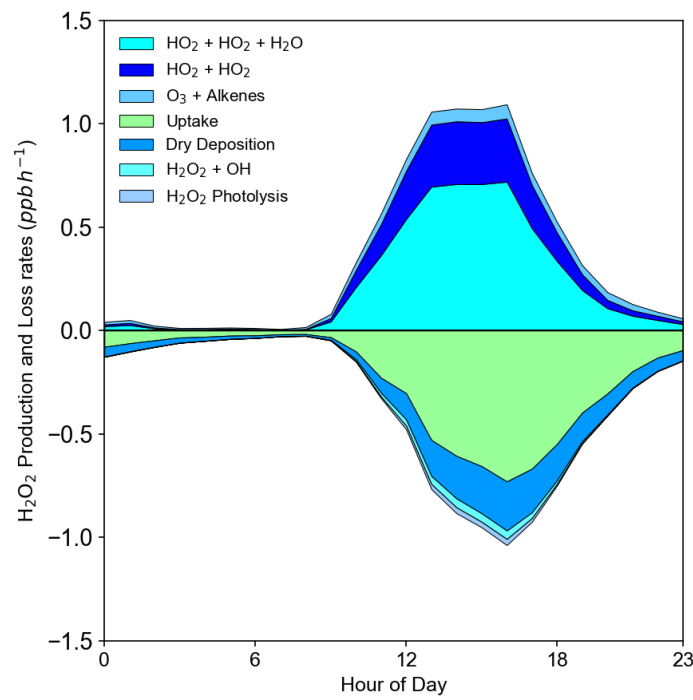


Figure 7. Modelled H₂O₂ sources and sinks.

Figure 7 depicts the H₂O₂ production rates and removal rates by different pathways. The percentage contribution of different pathways is shown in Figure S2. HO₂ bimolecular recombination was identified as the dominant H₂O₂ production pathway, contributing to 80% H₂O₂ production with a maximum yield of 1.0 ppb h⁻¹ at noon. This highlighted rapid photochemical production as the primary driver of H₂O₂ pollution in the rural site. In contrast, the reaction of O₃ with alkenes accounted for 9% H₂O₂ production (Figure S2), with a maximum yield of 0.07 ppb h⁻¹, primarily from O₃+OLI reactions. This mechanism was found to be significant during winter pollution due to high alkenes and NO concentrations inhibiting HO₂ recombination (Qin et al., 2018). Heterogeneous uptake dominated H₂O₂ removal, accounting for 64.69% with a maximum removal rate of

0.7 ppb h⁻¹, underscoring its importance during summer pollution periods. Dry deposition, photolysis, and reaction with OH radicals contributed to 25%, ~~42~~⁴²%, and ~~34~~³⁴% H₂O₂ loss, respectively. These findings provide a comprehensive understanding of H₂O₂ sources and sinks in rural environments, emphasizing the critical role of particle uptake in H₂O₂ budget.

3.5 Precursors control to mitigate H₂O₂ pollution

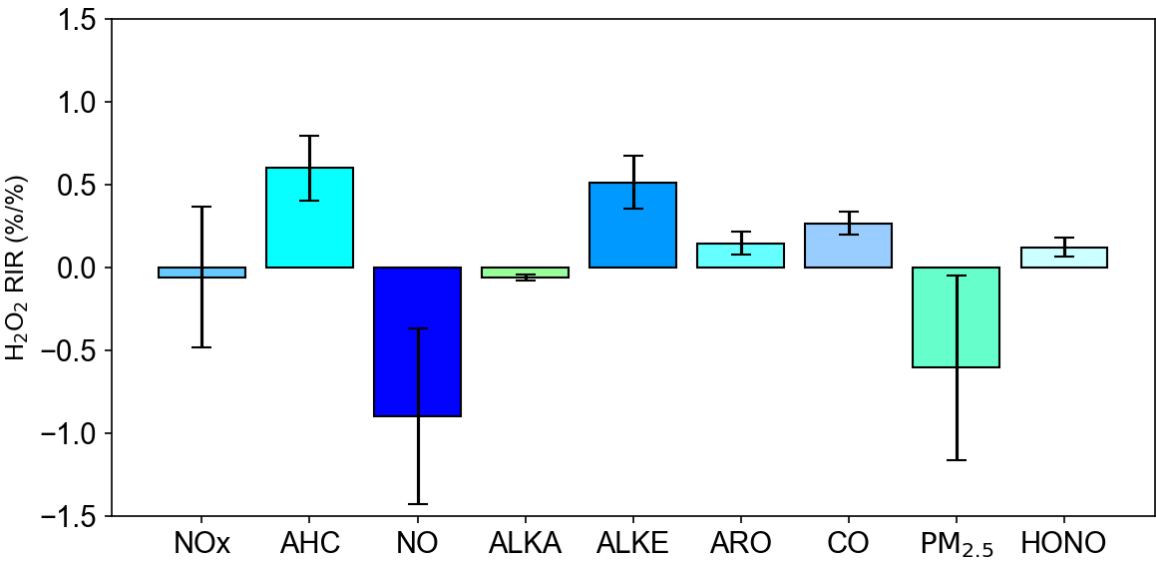


Figure 8. Sensitivity of H₂O₂ production to different chemical species.

It is evident that photochemical pollution in rural areas is associated with elevated concentrations of H₂O₂, necessitating urgent measures to mitigate H₂O₂ pollution by regulating its precursor compounds. Given the diversity of precursors involved in H₂O₂ formation, a critical objective is to quantify the relative contribution of each precursor to H₂O₂ pollution to establish prioritized control strategies. In this study, the RIR method was employed to identify the most effective pollutants for H₂O₂ control (Figure 8). Here it should be noted that the RIR analysis was performed using the adjusted model with H₂O₂ uptake coefficient of 6×10⁻⁴ that showed good agreement with observations. The results demonstrate that reducing NO concentrations leads to an increase in H₂O₂ levels, as the reaction between NO and HO₂ inhibits H₂O₂ production. However, under realistic conditions, a decrease in NO also results in reduced NO₂ levels. Since the NO₂ heterogeneous reaction is a significant source of HONO, which serves as a key precursor for OH influencing H₂O₂ formation, a decline in NO₂ consequently reduces H₂O₂ concentrations. To validate this hypothesis, RIR values for NOx were calculated. Although the absolute RIR values for NOx remained negative (-0.06), they were significantly lower than those for NO (-0.9), indicating that the reduction in H₂O₂ due to decreased NO₂ partially offsets the increase in H₂O₂ caused by reduced NO.

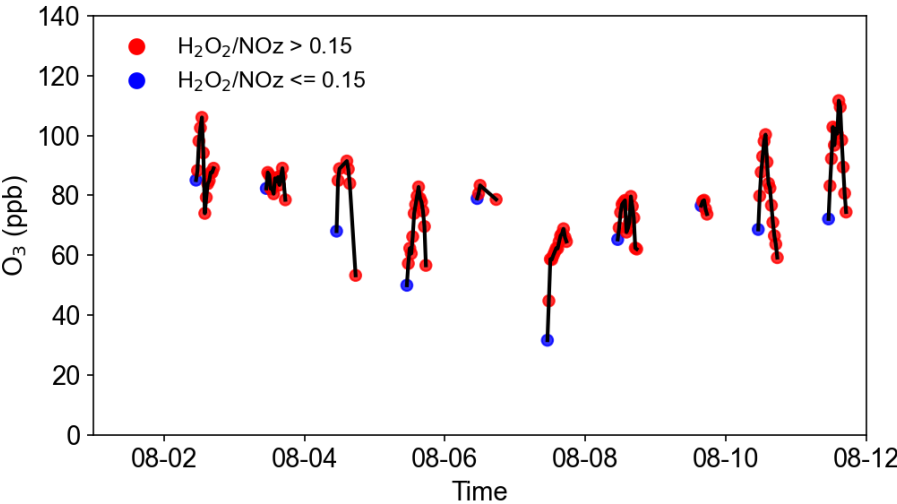
Furthermore, the negative RIR value for alkanes (-0.06) suggests that lowering alkane concentrations enhances H₂O₂ production, likely due to their lower photochemical reactivities with OH. When alkane levels are reduced, OH radicals preferentially react with more reactive alkenes and aromatics, leading to increased HO₂ and hence more H₂O₂ formation. The RIR values for alkenes (0.51), aromatics (0.15), and CO (0.26) were consistently positive, indicating that reducing these pollutants is effective in reducing H₂O₂ concentrations, with alkenes exhibiting the most pronounced effect. Consequently, controlling alkenes concentrations within anthropogenic VOCs should be prioritized, aligning with findings from previous studies (Wang et al., 2016; Ye et al., 2021a). Coal combustion and gasoline exhaust were identified as primary sources of alkenes in the region, underscoring the importance of regulating these emissions to mitigate H₂O₂ pollution. Additionally, RIR value for HONO was 0.12, indicating reducing HONO concentrations can further diminish H₂O₂ levels by limiting the primary radical source. Elevated HONO concentrations have been observed across various sites in China, contributing over 40% to primary radical production. Thus, reducing HONO emissions represents a potential mitigating strategy for H₂O₂. Ye et al. (2022) reported that HONO emissions due to fertilizer use significantly increase H₂O₂ levels in rural areas, suggesting that reducing excessive fertilizer use could mitigate H₂O₂ pollution. Moreover, NO₂ heterogeneous reactions at various interfaces and nitrate photolysis are additional sources of HONO (Xue et al., 2020; Xue et al., 2022), highlighting the potential to reduce H₂O₂ by decreasing NO₂ concentrations and subsequently limiting HONO production.

The RIR value for PM_{2.5} (-0.6) was found to be negative, as reducing PM_{2.5} decreases the uptake of H₂O₂, thereby increasing its gas-phase concentration. Recent studies have extensively examined the impact of PM_{2.5} reduction on O₃ concentrations, attributing this phenomenon to diminished HO₂ radical uptake and enhanced photolysis rates, both of which elevate O₃ levels (Wang et al., 2019; Song et al., 2022). These mechanisms similarly contribute to increased H₂O₂ concentrations, yet the effect of particulate matter reduction on H₂O₂ has been largely overlooked. This study demonstrates that PM_{2.5} reduction also decreases H₂O₂ uptake, further exacerbating its gas-phase concentration. This increase in H₂O₂ could enhance sulfate formation efficiency and pose greater threats to human health and ecosystems. Given the critical role of H₂O₂ in atmospheric oxidation capacity, global sulfate aerosol formation, and human health, further research is warranted to investigate H₂O₂ trends, environmental impacts, and mitigation strategies.

3.6 Implications on O₃ formation

H₂O₂ measurements serve as a valuable indicator of O₃ production sensitivity. Under NO_x poor conditions, the HO₂ recombination to form H₂O₂ represents the primary radical termination pathway. Conversely, under NO_x sufficient conditions, the reaction between NO₂ and OH to form nitric acid (HNO₃) constitutes the dominant termination mechanism. Sillman (1995) identified the H₂O₂/HNO₃ ratio as a robust indicator of O₃ sensitivity, with model simulations revealing that a ratio between 0.2 and 0.3 corresponds to a transitional regime, while values exceeding 0.3 indicate NO_x-limited conditions and values below 0.2 suggest VOC-limited conditions. In the absence of direct gaseous HNO₃ measurements, alternative

metrics such as $\text{H}_2\text{O}_2/\text{NO}_y$ or $\text{H}_2\text{O}_2/\text{NO}_z$ can be employed to assess O_3 sensitivity (Sillman et al., 1998), where NO_z encompasses HNO_3 , PAN, HONO, and alkyl nitrates, and NO_y is defined as $\text{NO}_z + \text{NO}_x$.



405

Figure 9. O_3 concentrations values from 1 August to 11 August. The red points represent measurements where $\text{H}_2\text{O}_2/\text{NO}_z$ is greater than 0.15, while the blue points correspond to measurements where $\text{H}_2\text{O}_2/\text{NO}_z$ is less than or equal to 0.15.

In this study, simultaneous measurements of H_2O_2 and NO_z enabled the determination of O_3 sensitivity using the $\text{H}_2\text{O}_2/\text{NO}_z$ ratio, with a transitional range identified at 0.15–0.20 (Sillman et al., 1998). The analysis focused on the period of intense photochemical activity between 10:00 and 17:00. As illustrated in Figure 9, over 82% of measured $\text{H}_2\text{O}_2/\text{NO}_z$ values exceeded 0.15, indicating that the rural study area predominantly exhibited NO_x -limited or transitional conditions during most of the observed period. It is important to note that this metric can be influenced by additional factors. For instance, significant uptake of H_2O_2 by particles was observed in this study, suggesting that the actual photochemical production of H_2O_2 is higher than the measured concentrations. Consequently, the theoretical $\text{H}_2\text{O}_2/\text{NO}_z$ ratio is likely greater than the observed values, implying that O_3 production is more strongly aligned with NO_x -limited or transitional regimes.

415

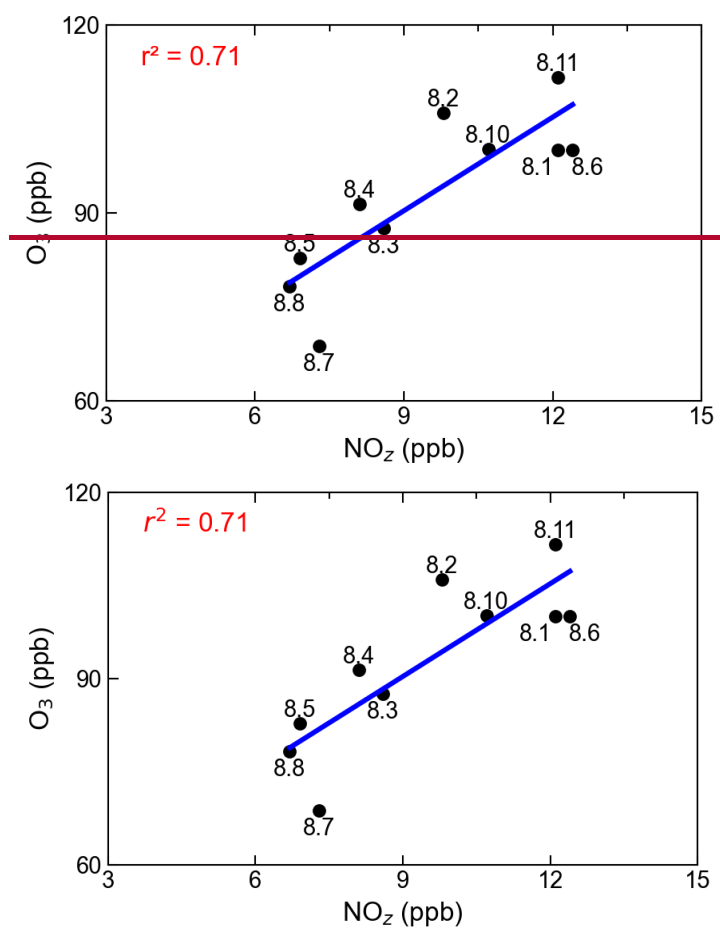


Figure 10. Correlation between daily maxima of O_3 and NO_z . The numbers adjacent to the solid dots represent the dates.

To corroborate these findings, the O_3/NO_z ratio was also utilized to evaluate O_3 sensitivity. The relationship between peak O_3 concentrations and peak NO_z concentrations demonstrated a good positive correlation ($r^2=0.71$), with a regression slope of 4.98. This slope is comparable with the value (3.3-7.6) reported in a mountainous area north of Beijing (Wang et al., 2006), but lower than those (6-11) observed in Houston (Daum et al., 2004). Notably, the positive correlation persisted up to NO_z concentrations of 12 ppb, differing from observations at other sites where the slope typically decreased for NO_z levels above 10 ppb (Trainer et al., 1993). This deviation can be attributed to reduced O_3 production efficiency under VOC-limited conditions. However, the sustained positive correlation across the entire study period suggests that the generation of NO_z is consistently accompanied by O_3 production, further supporting the prevalence of NO_x -sensitive or transitional regimes. These results align with those derived from the $\text{H}_2\text{O}_2/\text{NO}_z$ ratio, affirming the utility of $\text{H}_2\text{O}_2/\text{NO}_z$ as a reliable indicator of O_3 sensitivity.

The findings underscore the importance of controlling NO_x concentrations to mitigate photochemical pollution in rural areas. Tan et al. similarly reported that O₃ production in the rural North China Plain is primarily NO_x-limited. As NO_x emissions continue to decline due to regulatory efforts, an increasing number of regions may transition into NO_x-limited or transitional regimes, highlighting the potential benefits of stringent NO_x reduction strategies for future O₃ pollution control. However, given the need for synergistic management of H₂O₂ and O₃, a dual approach targeting both NO_x and VOC emissions remains essential. This integrated strategy will be critical for achieving effective and sustainable air quality improvements.

4 Conclusions

To investigate photochemical pollution in rural areas, measurements of H₂O₂ and related parameters were conducted in the Wangdu region during the summer of 2016. H₂O₂ exhibited a distinct diurnal pattern, with an average concentration of 0.62±0.80 ppb. Daily maximum concentrations of H₂O₂ varied significantly, ranging from a minimum of 0.2 ppb to a maximum of 4 ppb. The diurnal cycles of H₂O₂, PAN, and O₃ all followed solar radiation trends, indicating that photochemical reactions predominantly control their production. A good correlation ($r^2 = 0.55$) was observed between daily maximum concentrations of PAN and O₃, whereas the correlation between maximum concentrations of H₂O₂ and O₃ was weak, suggesting that unidentified processes influencing gas-phase H₂O₂ concentrations may attenuate this relationship. Analysis of the O₃/H₂O₂ ratio revealed that this ratio was significantly higher on polluted days compared to clean days, implying that particle uptake likely reduces gas-phase H₂O₂ concentrations.

To further elucidate the factors influencing H₂O₂ concentrations, a box model was employed. The model simulations initially overestimated H₂O₂ concentrations with a modelled-to-observed ratio of 2.7. However, when H₂O₂ heterogeneous uptake mechanism was incorporated into the model scheme with an uptake coefficient of 6×10^{-4} , the simulated H₂O₂ concentrations aligned well with observed data, underscoring the significant role of heterogeneous uptake in H₂O₂ removal. The primary source of H₂O₂ was identified as the bimolecular recombination of HO₂, contributing 91% of the total source strength, with a maximum production rate of 1 ppb h⁻¹. The dominant removal pathways for H₂O₂ included particle uptake (69%), followed by dry deposition (25%), reaction with OH (4%), and photolysis (2%).

Relative Incremental Reactivity (RIR) analysis demonstrated that reducing NO_x, PM_{2.5}, and alkanes exacerbated H₂O₂ concentrations, whereas lowering alkenes, aromatics, CO, and HONO effectively reduced H₂O₂ pollution, with alkenes exhibiting the most pronounced impact. The H₂O₂/NO_z ratio and the positive correlation between daily peak O₃ and NO_z concentrations indicated that O₃ production predominantly occurred in transitional and NO_x-limited regimes. To concurrently mitigate H₂O₂ and O₃ pollution, a dual strategy focusing on VOC control and stringent NO_x reduction is essential. This approach will be critical for achieving synergistic control of photochemical pollutants in rural areas.

Future research should focus on long-term H₂O₂ monitoring across different environments in the region, refining the parameterization of heterogeneous uptake processes (particularly for HO₂ and H₂O₂ under varying aerosol compositions), and investigating the impacts of changing VOC/NO_x ratios on H₂O₂ chemistry. In addition, further research on the interactions between gas-phase oxidants and aerosol processes will be vital for understanding the complex feedback mechanisms that influence air quality in rural and urban environments.

Data availability. The data used in this study are available from the corresponding author upon request (yjmu@rcees.ac.cn).

Author contributions. YM designed the experiments. CY performed H₂O₂ measurements and analyzed the data. CY wrote the manuscript with input from PL and CX. All authors contributed to measurements, discussing results, and commenting on the manuscript.

Competing interests. The contact author has declared that neither they nor their co-authors have any competing interests.

Acknowledgements. We thank the science teams of the summer campaign for their support.

Financial support. This work was supported by the National Natural Science Foundation of China (grant nos. 42305099, 42275111).

References

Allen, H. M., Bates, K. H., Crounse, J. D., Kim, M. J., Teng, A. P., Ray, E. A., and Wennberg, P. O.: H₂O₂ and CH₃OOH (MHP) in the Remote Atmosphere: 2. Physical and Chemical Controls, *Journal of Geophysical Research: Atmospheres*, 127, e2021JD035702, <https://doi.org/10.1029/2021JD035702>, 2022.

Ayers, G., Penkett, S., Gillett, R., Bandy, B., Galbally, I., Meyer, C., Elsworth, C., Bentley, S., and Forgan, B.: Evidence for photochemical control of ozone concentrations in unpolluted marine air, *Nature*, 360, 446-449, 1992.

Balasubramanian, R. and Husain, L.: Observations of gas-phase hydrogen peroxide at an elevated rural site in New York, *J Geophys Res-Atmos*, 102, 21209-21220, Doi 10.1029/97jd01480, 1997.

Becker, K. H., Brockmann, K. J., and Bechara, J.: Production of hydrogen peroxide in forest air by reaction of ozone with terpenes, *Nature*, 346, 256-258, 1990.

Calvert, J. G., Lazrus, A., Kok, G. L., Heikes, B. G., Walega, J. G., Lind, J., and Cantrell, C. A.: Chemical Mechanisms of Acid Generation in the Troposphere, *Nature*, 317, 27-35, Doi 10.1038/317027a0, 1985.

Chen, X., Aoki, M., Takami, A., Chai, F., and Hatakeyama, S.: Effect of ambient-level gas-phase peroxides on foliar injury, growth, and net photosynthesis in Japanese radish (*Raphanus sativus*), *Environ Pollut*, 158, 1675-1679, 10.1016/j.envpol.2009.12.002, 2010.

Daum, P. H., Kleinman, L. I., Springston, S. R., Nunnermacker, L. J., Lee, Y. N., Weinstein-Lloyd, J., Zheng, J., and Berkowitz, C. M.: Origin and properties of plumes of high ozone observed during the Texas 2000 Air Quality Study (TexAQS 2000), *Journal of Geophysical Research: Atmospheres*, 109, <https://doi.org/10.1029/2003JD004311>, 2004.

de Reus, M., Fischer, H., Sander, R., Gros, V., Kormann, R., Salisbury, G., Van Dingenen, R., Williams, J., Zöllner, M., and Lelieveld, J.: Observations and model calculations of trace gas scavenging in a dense Saharan dust plume during MINATROC, *Atmos. Chem. Phys.*, 5, 1787-1803, 10.5194/acp-5-1787-2005, 2005.

Fischer, H., Pozzer, A., Schmitt, T., Jöckel, P., Klippel, T., Taraborrelli, D., and Lelieveld, J.: Hydrogen peroxide in the marine boundary layer over the South Atlantic during the OOMPH cruise in March 2007, *Atmos Chem Phys*, 15, 6971-6980, 2015.

510 Fischer, H., Axinte, R., Bozem, H., Crowley, J. N., Ernest, C., Gilge, S., Hafermann, S., Harder, H., Hens, K., and Janssen, R. H.: Diurnal variability, photochemical production and loss processes of hydrogen peroxide in the boundary layer over Europe, *Atmos Chem Phys*, 19, 11953-11968, 2019.

515 Gao, J., Wang, H., Liu, W., Xu, H., Wei, Y., Tian, X., Feng, Y., Song, S., and Shi, G.: Hydrogen peroxide serves as pivotal fountainhead for aerosol aqueous sulfate formation from a global perspective, *Nat Commun*, 15, 4625, 10.1038/s41467-024-48793-1, 2024.

520 George, I. J., Matthews, P. S. J., Whalley, L. K., Brooks, B., Goddard, A., Baeza-Romero, M. T., and Heard, D. E.: Measurements of uptake coefficients for heterogeneous loss of HO₂ onto submicron inorganic salt aerosols, *Phys Chem Chem Phys*, 15, 12829-12845, 10.1039/C3CP51831K, 2013.

Guo, J., Wang, Z., Cui, Y., and Zhang, X.: Assessment of the H₂O₂ budget at an urban site concerning the HO₂ underprediction and the vertical transport from residual layers, *Atmos Environ*, 272, 118952, <https://doi.org/10.1016/j.atmosenv.2022.118952>, 2022.

525 Guo, J., Tilgner, A., Yeung, C., Wang, Z., Louie, P. K. K., Luk, C. W. Y., Xu, Z., Yuan, C., Gao, Y., Poon, S., Herrmann, H., Lee, S., Lam, K. S., and Wang, T.: Atmospheric Peroxides in a Polluted Subtropical Environment: Seasonal Variation, Sources and Sinks, and Importance of Heterogeneous Processes, *Environ Sci Technol*, 48, 1443-1450, 10.1021/es403229x, 2014.

530 He, S. Z., Chen, Z. M., Zhang, X., Zhao, Y., Huang, D. M., Zhao, J. N., Zhu, T., Hu, M., and Zeng, L. M.: Measurement of atmospheric hydrogen peroxide and organic peroxides in Beijing before and during the 2008 Olympic Games: Chemical and physical factors influencing their concentrations, *J Geophys Res-Atmos*, 115, ArtD17307, 10.1029/2009jd013544, 2010.

535 Hua, W., Chen, Z. M., Jie, C. Y., Kondo, Y., Hofzumahaus, A., Takegawa, N., Chang, C. C., Lu, K. D., Miyazaki, Y., Kita, K., Wang, H. L., Zhang, Y. H., and Hu, M.: Atmospheric hydrogen peroxide and organic hydroperoxides during PRIDE-PRD'06, China: their concentration, formation mechanism and contribution to secondary aerosols, *Atmos Chem Phys*, 8, 6755-6773, DOI 10.5194/acp-8-6755-2008, 2008.

540 Kanaya, Y., Cao, R., Akimoto, H., Fukuda, M., Komazaki, Y., Yokouchi, Y., Koike, M., Tanimoto, H., Takegawa, N., and Kondo, Y.: Urban photochemistry in central Tokyo: 1. Observed and modeled OH and HO₂ radical concentrations during the winter and summer of 2004, *Journal of Geophysical Research: Atmospheres*, 112, <https://doi.org/10.1029/2007JD008670>, 2007a.

545 Kanaya, Y., Tanimoto, H., Matsumoto, J., Furutani, H., Hashimoto, S., Komazaki, Y., Tanaka, S., Yokouchi, Y., Kato, S., Kajii, Y., and Akimoto, H.: Diurnal variations in H₂O₂, O₃, PAN, HNO₃ and aldehyde concentrations and NO/NO₂ ratios at Rishiri Island, Japan: Potential influence from iodine chemistry, *Sci Total Environ*, 376, 185-197, <https://doi.org/10.1016/j.scitotenv.2007.01.073>, 2007b.

550 Klippel, T., Fischer, H., Bozem, H., Lawrence, M. G., Butler, T., Jöckel, P., Tost, H., Martinez, M., Harder, H., and Regelin, E.: Distribution of hydrogen peroxide, methyl hydroperoxide and formaldehyde over central Europe during the HOOVER project, *Atmos Chem Phys*, 11, 4391-4410, 2011.

- 555 Lakey, P. S. J., George, I. J., Whalley, L. K., Baeza-Romero, M. T., and Heard, D. E.: Measurements of the HO₂ Uptake Coefficients onto Single Component Organic Aerosols, *Environ Sci Technol*, 49, 4878-4885, 10.1021/acs.est.5b00948, 2015.
- Lazrus, A. L., Kok, G. L., Lind, J. A., Gitlin, S. N., Heikes, B. G., and Shetter, R. E.: Automated Fluorometric Method for Hydrogen-Peroxide in Air, *Anal Chem*, 58, 594-597, Doi 10.1021/Ac00294a024, 1986.
- 560 Lee, G., Jang, Y., Lee, H., Han, J.-S., Kim, K.-R., and Lee, M.: Characteristic behavior of peroxyacetyl nitrate (PAN) in Seoul megacity, Korea, *Chemosphere*, 73, 619-628, <https://doi.org/10.1016/j.chemosphere.2008.05.060>, 2008a.
- Lee, M., Kie, J. A., Kim, Y. M., and Lee, G.: Characteristics of atmospheric hydrogen peroxide variations in Seoul megacity during 2002-2004, *Sci Total Environ*, 393, 299-308, 10.1016/j.scitotenv.2007.11.037, 2008b.
- 565 Li, J. R., Zhu, C., Chen, H., Fu, H. B., Xiao, H., Wang, X. F., Herrmann, H., and Chen, J. M.: A More Important Role for the Ozone-S(IV) Oxidation Pathway Due to Decreasing Acidity in Clouds, *J Geophys Res-Atmos*, 125, 2020.
- 570 Li, K., Jacob, D. J., Liao, H., Shen, L., Zhang, Q., and Bates, K. H.: Anthropogenic drivers of 2013-2017 trends in summer surface ozone in China, *P Natl Acad Sci USA*, 116, 422-427, 10.1073/pnas.1812168116, 2019.
- Liang, H., Chen, Z. M., Huang, D., Zhao, Y., and Li, Z. Y.: Impacts of aerosols on the chemistry of atmospheric trace gases: a case study of peroxides and HO₂ radicals, *Atmos Chem Phys*, 13, 11259-11276, 10.5194/acp-13-11259-2013, 2013.
- 575 Liu, P., Ye, C., Zhang, C., He, G., Xue, C., Liu, J., Liu, C., Zhang, Y., Song, Y., Li, X., Wang, X., Chen, J., He, H., Herrmann, H., and Mu, Y.: Photochemical Aging of Atmospheric Fine Particles as a Potential Source for Gas-Phase Hydrogen Peroxide, *Environ Sci Technol*, 55, 15063-15071, 10.1021/acs.est.1c04453, 2021.
- 580 Liu, Y., Geng, G., Cheng, J., Liu, Y., Xiao, Q., Liu, L., Shi, Q., Tong, D., He, K., and Zhang, Q.: Drivers of Increasing Ozone during the Two Phases of Clean Air Actions in China 2013–2020, *Environ Sci Technol*, 57, 8954-8964, 10.1021/acs.est.3c00054, 2023.
- 585 Lu, X., Zhang, L., Wang, X., Gao, M., Li, K., Zhang, Y., Yue, X., and Zhang, Y.: Rapid Increases in Warm-Season Surface Ozone and Resulting Health Impact in China Since 2013, *Environmental Science & Technology Letters*, 7, 240-247, 2020.
- Ma, X., Tan, Z., Lu, K., Yang, X., Chen, X., Wang, H., Chen, S., Fang, X., Li, S., Li, X., Liu, J., Liu, Y., Lou, S., Qiu, W., Wang, H., Zeng, L., and Zhang, Y.: OH and HO₂ radical chemistry at a suburban site during the EXPLORE-YRD campaign in 2018, *Atmos. Chem. Phys.*, 22, 7005-7028, 10.5194/acp-22-7005-2022, 2022.
- 590 Ma, Z., Xu, J., Quan, W., Zhang, Z., Lin, W., and Xu, X.: Significant increase of surface ozone at a rural site, north of eastern China, *Atmos. Chem. Phys.*, 16, 3969-3977, 10.5194/acp-16-3969-2016, 2016.
- 595 Nunnermacker, L. J., Weinstein-Lloyd, J. B., Hillery, B., Giebel, B., Kleinman, L. I., Springston, S. R., Daum, P. H., Gaffney, J., Marley, N., and Huey, G.: Aircraft and ground-based measurements of hydroperoxides during the 2006 MILAGRO field campaign, *Atmos Chem Phys*, 8, 7619-7636, 10.5194/acp-8-7619-2008, 2008.
- 600 Peng, X., Wang, W., Xia, M., Chen, H., Ravishankara, A. R., Li, Q., Saiz-Lopez, A., Liu, P., Zhang, F., Zhang, C., Xue, L., Wang, X., George, C., Wang, J., Mu, Y., Chen, J., and Wang, T.: An unexpected large continental source of reactive bromine and chlorine with significant impact on wintertime air quality, *National Science Review*, 8, nwaa304, 10.1093/nsr/nwaa304, 2021.

- Penkett, S. A., Jones, B. M. R., Brice, K. A., and Eggleton, A. E. J.: Importance of Atmospheric Ozone and Hydrogen-Peroxide in Oxidizing Sulfur-Dioxide in Cloud and Rainwater, *Atmos Environ*, 13, 123-137, Doi 10.1016/0004-6981(79)90251-8, 1979.
- Pradhan, M., Kalberer, M., Griffiths, P. T., Braban, C. F., Pope, F. D., Cox, R. A., and Lambert, R. M.: Uptake of Gaseous Hydrogen Peroxide by Submicrometer Titanium Dioxide Aerosol as a Function of Relative Humidity, *Environ Sci Technol*, 44, 1360-1365, 10.1021/es902916f, 2010.
- Qin, M., Chen, Z., Shen, H., Li, H., Wu, H., and Wang, Y.: Impacts of heterogeneous reactions to atmospheric peroxides: Observations and budget analysis study, *Atmos Environ*, 183, 144-153, 10.1016/j.atmosenv.2018.04.005, 2018.
- Qin, X., Chen, Z., Gong, Y., Dong, P., Cao, Z., Hu, J., and Xu, J.: Persistent Uptake of H₂O₂ onto Ambient PM_{2.5} via Dark-Fenton Chemistry, *Environ Sci Technol*, 56, 9978-9987, 10.1021/acs.est.2c03630, 2022.
- Rao, Z., Fang, Y.-G., Pan, Y., Yu, W., Chen, B., Francisco, J. S., Zhu, C., and Chu, C.: Accelerated Photolysis of H₂O₂ at the Air–Water Interface of a Microdroplet, *Journal of the American Chemical Society*, 145, 24717-24723, 10.1021/jacs.3c08101, 2023.
- Reeves, C. E. and Penkett, S. A.: Measurements of peroxides and what they tell us, *Chem Rev*, 103, 5199-5218, 10.1021/cr0205053, 2003.
- Ren, Y., Ding, A. J., Wang, T., Shen, X. H., Guo, J., Zhang, J. M., Wang, Y., Xu, P. J., Wang, X. F., Gao, J., and Collett, J. L.: Measurement of gas-phase total peroxides at the summit of Mount Tai in China, *Atmos Environ*, 43, 1702-1711, 10.1016/j.atmosenv.2008.12.020, 2009.
- Romanias, M. N., El Zein, A., and Bedjanian, Y.: Heterogeneous Interaction of H₂O₂ with TiO₂ Surface under Dark and UV Light Irradiation Conditions, *The Journal of Physical Chemistry A*, 116, 8191-8200, 10.1021/jp305366v, 2012.
- Sillman, S.: The use of NO_y, H₂O₂, and HNO₃ as indicators for ozone-NO_x-hydrocarbon sensitivity in urban locations, *Journal of Geophysical Research: Atmospheres*, 100, 14175-14188, 1995.
- Sillman, S., He, D., Pippin, M. R., Daum, P. H., Imre, D. G., Kleinman, L. I., Lee, J. H., and Weinstein-Lloyd, J.: Model correlations for ozone, reactive nitrogen, and peroxides for Nashville in comparison with measurements: Implications for O₃-NO_x-hydrocarbon chemistry, *Journal of Geophysical Research: Atmospheres*, 103, 22629-22644, 1998.
- Sofen, E. D., Alexander, B., and Kunasek, S. A.: The impact of anthropogenic emissions on atmospheric sulfate production pathways, oxidants, and ice core $\Delta\text{O}^{17}(\text{SO}_4^{2-})$, *Atmos. Chem. Phys.*, 11, 3565-3578, 10.5194/acp-11-3565-2011, 2011.
- Song, H., Lu, K., Dong, H., Tan, Z., Chen, S., Zeng, L., and Zhang, Y.: Reduced Aerosol Uptake of Hydroperoxyl Radical May Increase the Sensitivity of Ozone Production to Volatile Organic Compounds, *Environmental Science & Technology Letters*, 9, 22-29, 10.1021/acs.estlett.1c00893, 2022.
- Sun, M., Cui, J. n., Zhao, X., and Zhang, J.: Impacts of precursors on peroxyacetyl nitrate (PAN) and relative formation of PAN to ozone in a southwestern megacity of China, *Atmos Environ*, 231, 117542, <https://doi.org/10.1016/j.atmosenv.2020.117542>, 2020.
- Takami, A., Shiratori, N., Yonekura, H., and Hatakeyama, S.: Measurement of hydroperoxides and ozone in Oku-Nikko area, *Atmos Environ*, 37, 3861-3872, 10.1016/S1352-2310(03)00454-0, 2003.

- Taketani, F., Kanaya, Y., Pochanart, P., Liu, Y., Li, J., Okuzawa, K., Kawamura, K., Wang, Z., and Akimoto, H.: Measurement of overall uptake coefficients for HO₂ radicals by aerosol particles sampled from ambient air at Mts. Tai and Mang (China), *Atmos. Chem. Phys.*, 12, 11907-11916, 10.5194/acp-12-11907-2012, 2012.
- 655 Tan, Z., Hofzumahaus, A., Lu, K., Brown, S. S., Holland, F., Huey, L. G., Kiendler-Scharr, A., Li, X., Liu, X., Ma, N., Min, K.-E., Rohrer, F., Shao, M., Wahner, A., Wang, Y., Wiedensohler, A., Wu, Y., Wu, Z., Zeng, L., Zhang, Y., and Fuchs, H.: No Evidence for a Significant Impact of Heterogeneous Chemistry on Radical Concentrations in the North China Plain in Summer 2014, *Environ Sci Technol*, 54, 5973-5979, 10.1021/acs.est.0c00525, 2020.
- 660 Tan, Z., Fuchs, H., Lu, K., Hofzumahaus, A., Bohn, B., Broch, S., Dong, H., Gomm, S., Häsel, R., He, L., Holland, F., Li, X., Liu, Y., Lu, S., Rohrer, F., Shao, M., Wang, B., Wang, M., Wu, Y., Zeng, L., Zhang, Y., Wahner, A., and Zhang, Y.: Radical chemistry at a rural site (Wangdu) in the North China Plain: observation and model calculations of OH, HO₂ and RO₂ radicals, *Atmos. Chem. Phys.*, 17, 663-690, 10.5194/acp-17-663-2017, 2017.
- 665 Tang, M. J., Huang, X., Lu, K. D., Ge, M. F., Li, Y. J., Cheng, P., Zhu, T., Ding, A. J., Zhang, Y. H., Gligorovski, S., Song, W., Ding, X., Bi, X. H., and Wang, X. M.: Heterogeneous reactions of mineral dust aerosol: implications for tropospheric oxidation capacity, *Atmos Chem Phys*, 17, 11727-11777, 10.5194/acp-17-11727-2017, 2017.
- 670 Thornton, J. A., Jaeglé, L., and McNeill, V. F.: Assessing known pathways for HO₂ loss in aqueous atmospheric aerosols: Regional and global impacts on tropospheric oxidants, *Journal of Geophysical Research: Atmospheres*, 113, <https://doi.org/10.1029/2007JD009236>, 2008.
- 675 Trainer, M., Parrish, D. D., Buhr, M. P., Norton, R. B., Fehsenfeld, F. C., Anlauf, K. G., Bottenheim, J. W., Tang, Y. Z., Wiebe, H. A., Roberts, J. M., Tanner, R. L., Newman, L., Bowersox, V. C., Meagher, J. F., Olszyna, K. J., Rodgers, M. O., Wang, T., Berresheim, H., Demerjian, K. L., and Roychowdhury, U. K.: Correlation of ozone with NO_y in photochemically aged air, *Journal of Geophysical Research: Atmospheres*, 98, 2917-2925, <https://doi.org/10.1029/92JD01910>, 1993.
- 680 Walker, S. J., Evans, M. J., Jackson, A. V., Steinbacher, M., Zellweger, C., and McQuaid, J. B.: Processes controlling the concentration of hydroperoxides at Jungfraujoch Observatory, Switzerland, *Atmos Chem Phys*, 6, 5525-5536, DOI 10.5194/acp-6-5525-2006, 2006.
- 685 Wang, T., Ding, A., Gao, J., and Wu, W. S.: Strong ozone production in urban plumes from Beijing, China, *Geophys Res Lett*, 33, 2006.
- Wang, W., Li, X., Shao, M., Hu, M., Zeng, L., Wu, Y., and Tan, T.: The impact of aerosols on photolysis frequencies and ozone production in Beijing during the 4-year period 2012–2015, *Atmos. Chem. Phys.*, 19, 9413-9429, 10.5194/acp-19-9413-2019, 2019.
- 690 Wang, W., Parrish, D. D., Li, X., Shao, M., Liu, Y., Mo, Z., Lu, S., Hu, M., Fang, X., Wu, Y., Zeng, L., and Zhang, Y.: Exploring the drivers of the increased ozone production in Beijing in summertime during 2005–2016, *Atmos. Chem. Phys.*, 20, 15617-15633, 10.5194/acp-20-15617-2020, 2020.
- 695 Wang, Y., Chen, Z. M., Wu, Q. Q., Liang, H., Huang, L. B., Li, H., Lu, K. D., Wu, Y. S., Dong, H. B., Zeng, L. M., and Zhang, Y. H.: Observation of atmospheric peroxides during Wangdu Campaign 2014 at a rural site in the North China Plain, *Atmos Chem Phys*, 16, 10985-11000, 10.5194/acp-16-10985-2016, 2016.
- Watanabe, K., Yachi, C., Nishibe, M., Michigami, S., Saito, Y., Eda, N., Yamazaki, N., and Hirai, T.: Measurements of atmospheric hydroperoxides over a rural site in central Japan during summers using a helicopter, *Atmos Environ*, 146, 174-182, 2016.
- 700

- Watkins, B. A., Parrish, D. D., Buhr, S., Norton, R. B., Trainer, M., Yee, J. E., and Fehsenfeld, F. C.: Factors influencing the concentration of gas phase hydrogen peroxide during the summer at Kinterbish, Alabama, *Journal of Geophysical Research: Atmospheres*, 100, 22841-22851, <https://doi.org/10.1029/95JD01533>, 1995.
- 705 Whalley, L. K., Furneaux, K. L., Goddard, A., Lee, J. D., Mahajan, A., Oetjen, H., Read, K. A., Kaaden, N., Carpenter, L. J., Lewis, A. C., Plane, J. M. C., Saltzman, E. S., Wiedensohler, A., and Heard, D. E.: The chemistry of OH and HO₂ radicals in the boundary layer over the tropical Atlantic Ocean, *Atmos. Chem. Phys.*, 10, 1555-1576, 10.5194/acp-10-1555-2010, 2010.
- 710 Xu, W., Zhang, G., Wang, Y., Tong, S., Zhang, W., Ma, Z., Lin, W., Kuang, Y., Yin, L., and Xu, X.: Aerosol Promotes Peroxyacetyl Nitrate Formation During Winter in the North China Plain, *Environ Sci Technol*, 55, 3568-3581, 10.1021/acs.est.0c08157, 2021.
- 715 Xue, C., Ye, C., Kleffmann, J., Zhang, W., He, X., Liu, P., Zhang, C., Zhao, X., Liu, C., Ma, Z., Liu, J., Wang, J., Lu, K., Catoire, V., Mellouki, A., and Mu, Y.: Atmospheric measurements at Mt. Tai – Part II: HONO budget and radical (RO_x+NO₃) chemistry in the lower boundary layer, *Atmos. Chem. Phys.*, 22, 1035-1057, 10.5194/acp-22-1035-2022, 2022.
- 720 Xue, C. Y., Zhang, C. L., Ye, C., Liu, P. F., Catoire, V., Krysztofiak, G., Chen, H., Ren, Y. G., Zhao, X. X., Wang, J. H., Zhang, F., Zhang, C. X., Zhang, J. W., An, J. L., Wang, T., Chen, J. M., Kleffmann, J., Mellouki, A., and Mu, Y. J.: HONO Budget and Its Role in Nitrate Formation in the Rural North China Plain, *Environ Sci Technol*, 54, 11048-11057, 2020.
- 725 Ye, C., Liu, P., Ma, Z., Xue, C., Zhang, C., Zhang, Y., Liu, J., Liu, C., Sun, X., and Mu, Y.: High H₂O₂ Concentrations Observed during Haze Periods during the Winter in Beijing: Importance of H₂O₂ Oxidation in Sulfate Formation, *Environmental Science & Technology Letters*, 10.1021/acs.estlett.8b00579, 2018.
- Ye, C., Xue, C., Liu, P., Zhang, C., Ma, Z., Zhang, Y., Liu, C., Liu, J., Lu, K., and Mu, Y.: Strong impacts of biomass burning, nitrogen fertilization, and fine particles on gas-phase hydrogen peroxide (H₂O₂), *Sci Total Environ*, 843, 156997, <https://doi.org/10.1016/j.scitotenv.2022.156997>, 2022.
- 730 Ye, C., Xue, C., Zhang, C., Ma, Z., Liu, P., Zhang, Y., Liu, C., Zhao, X., Zhang, W., He, X., Song, Y., Liu, J., Wang, W., Sui, B., Cui, R., Yang, X., Mei, R., Chen, J., and Mu, Y.: Atmospheric Hydrogen Peroxide (H₂O₂) at the Foot and Summit of Mt. Tai: Variations, Sources and Sinks, and Implications for Ozone Formation Chemistry, *Journal of Geophysical Research: Atmospheres*, 126, e2020JD033975, <https://doi.org/10.1029/2020JD033975>, 2021a.
- 735 Ye, C., Chen, H., Hoffmann, E. H., Mettke, P., Tilgner, A., He, L., Mutzel, A., Brüggemann, M., Poulain, L., Schaefer, T., Heinold, B., Ma, Z., Liu, P., Xue, C., Zhao, X., Zhang, C., Zhang, F., Sun, H., Li, Q., Wang, L., Yang, X., Wang, J., Liu, C., Xing, C., Mu, Y., Chen, J., and Herrmann, H.: Particle-Phase Photoreactions of HULIS and TMIs Establish a Strong Source of H₂O₂ and Particulate Sulfate in the Winter North China Plain, *Environ Sci Technol*, 55, 7818-7830, 10.1021/acs.est.1c00561, 2021b.
- 740 Zhang, G., Mu, Y. J., Liu, J. F., Zhang, C. L., Zhang, Y. Y., Zhang, Y. J., and Zhang, H. X.: Seasonal and diurnal variations of atmospheric peroxyacetyl nitrate, peroxypropionyl nitrate, and carbon tetrachloride in Beijing, *J Environ Sci-China*, 26, 65-74, 10.1016/S1001-0742(13)60382-4, 2014.
- 745 Zhang, Q., Liu, J., He, Y., Yang, J., Gao, J., Liu, H., Tang, W., Chen, Y., Fan, W., Chen, X., Chai, F., and Hatakeyama, S.: Measurement of hydrogen peroxide and organic hydroperoxide concentrations during autumn in Beijing, China, *J Environ Sci-China*, 64, 72-81, <https://doi.org/10.1016/j.jes.2016.12.015>, 2018.

750 Zhang, X., He, S. Z., Chen, Z. M., Zhao, Y., and Hua, W.: Methyl hydroperoxide (CH₃OOH) in urban, suburban and rural atmosphere: ambient concentration, budget, and contribution to the atmospheric oxidizing capacity, *Atmos. Chem. Phys.*, 12, 8951-8962, 10.5194/acp-12-8951-2012, 2012.